Line-shape analysis of Doppler-broadened γ lines following the β decay of ^{11}Li

C. M. Mattoon,[1,*] F. Sarazin,[1,†] C. Andreoiu,[2] A. N. Andreyev,[3,‡] R. A. E. Austin,[4] G. C. Ball,[3] R. S. Chakrawarthy,[3] D. Cross,[2] E. S. Cunningham,[3] J. Daoud,[3] P. E. Garrett,[5] G. F. Grinyer,[5,§] G. Hackman,[3] D. Melconian,[6,7] C. Morton,[3] C. Pearson,[3] J. J. Ressler,[2] J. Schwarzenberg,[8] M. B. Smith,[3,‖] and C. E. Svensson[5]

[1]*Department of Physics, Colorado School of Mines, Golden, CO 80401, USA*
[2]*Department of Chemistry, Simon Fraser University, Burnaby, BC, V5A 1S6, Canada*
[3]*TRIUMF, 4004 Wesbrook Mall, Vancouver, BC, V6T 2A3, Canada*
[4]*Department of Physics and Astronomy, Saint Mary's University, Halifax, NS, B3H 3C3, Canada*
[5]*Department of Physics, University of Guelph, Guelph, ON, N1G 2W1, Canada*
[6]*Department of Physics, Simon Fraser University, Burnaby, BC, V5A 1S6, Canada*
[7]*Department of Physics, Texas A&M, College Station, TX 77843, USA*
[8]*Department of Nuclear Physics, University of Vienna, Waehringerstrasse 17, AT-1090 Vienna, Austria*

(Received 19 June 2009; published 23 September 2009)

The β decay of ^{11}Li is studied at the TRIUMF Isotope Separation and Acceleration (ISAC) facility using the 8π γ-ray spectrometer coupled with an inner array of 20 plastic scintillators for β detection. Doppler-broadened line shapes resulting from the decay of the excited states in ^{10}Be populated by β-delayed one-neutron emission are analyzed using Monte Carlo simulations. New β-delayed neutron decay branches are shown to contribute to the complex decay of ^{11}Li. The half-lives of all but one bound excited state in ^{10}Be are also deduced from this work. Among them, the half-life of the 2^- state in ^{10}Be is shown to be much shorter than previously thought, yielding a new experimental $B(E1)$ now well within the range of theoretical predictions and providing further evidence that the 2^- state in ^{10}Be is an excited halo state. The nature of the 8.82-MeV state in ^{11}Be and its decay paths to excited states in ^{10}Be are found to be consistent with the β decay of the core proceeding through this particular state.

DOI: 10.1103/PhysRevC.80.034318 PACS number(s): 23.20.−g, 23.40.−s, 27.20.+n

I. INTRODUCTION

Over the years, ^{11}Li has emerged as having perhaps the most complex decay scheme among light nuclei. One reason, of course, lies in its large Q_β value (20.55 MeV), which opens a large number of possible decay channels. But another reason for such complexity can be found in the study of the β-delayed one-neutron emission where most of the ^{11}Li β-decay strength lies. Past experiments [1–6] show that multiple decay paths to ^{11}Be and ^{10}Be contribute to the decay, pointing to a lack of overlap between the ^{11}Li ground-state wave function and the ones making up the states in the daughter nucleus. This may not be particularly surprising if one considers the difference between the halo nature of the ^{11}Li ground state [7,8] and the clustered nature of many beryllium states (see Ref. [9] and references therein). However, two neutron-rich beryllium isotopes are known halo nuclei, and at least one excited state in ^{10}Be (2^- state at 6.263 MeV) has been identified as a halo state candidate (see Ref. [10] and references therein). Such a coexistence between halo and cluster structures in beryllium isotopes is intriguing and suggests that under certain conditions, the valence neutrons as described in cluster models may also be halo neutrons. Recently, two experiments at the TRIUMF Isotope Separation and Acceleration (ISAC) facility investigated decay paths that could shed light on the fate of the ^{11}Li halo neutrons. The measurement of the β-delayed deuteron channel is shown to occur mostly in the halo of ^{11}Li [11], while the study of the β-delayed neutron emission points to possible pathways consistent with the β decay occurring in the core [5]. In the latter case, one expects the halo neutrons to remain decoupled from the core and therefore to survive the β decay in a similar configuration in the daughter nucleus. One pathway described in Ref. [5] is especially striking, as the β-delayed neutron emission proceeds through the 8.82-MeV ($3/2^-$) excited state in ^{11}Be, a state with an apparent $^9\mathrm{Be} + n + n$ structure, and the 6.263-MeV (2^-) excited state in ^{10}Be mentioned above. In this case, not only do the two halo neutrons survive the β-decay process in the ^{11}Be intermediate state, but also one of them eventually survives the subsequent neutron emission to help form the 2^- excited halo state in ^{10}Be. Interestingly, the 8.82-MeV state in ^{10}Be is now proposed as a candidate for a molecular bandhead [12], suggesting that this state may precisely be a case in which halo and molecular structures coexist.

Furthermore, recent progress in *ab-initio* calculations now allow direct comparison of theoretical calculations, such as the no-core shell model (NCSM), with experimental data in light nuclei. In this context, ^{10}Be is perhaps one of the most interesting nuclei among the larger nuclei treated with this approach. Transition strengths, for example, are important

*Present Address: National Nuclear Data Center, Brookhaven National Laboratory, Upton, NY 11973, USA.
†Corresponding author: fsarazin@mines.edu
‡Present address: Instituut voor Kern- en Stralingsfysica, Katholieke Universiteit Leuven, BE-3001 Leuven, Belgium.
§Present address: National Superconducting Cyclotron Laboratory, Michigan State University, East Lansing, MI 48824, USA.
‖Present address: Bubble Technology Industries, P. O. Box 100, Chalk River, ON, K0J 1J0, Canada.

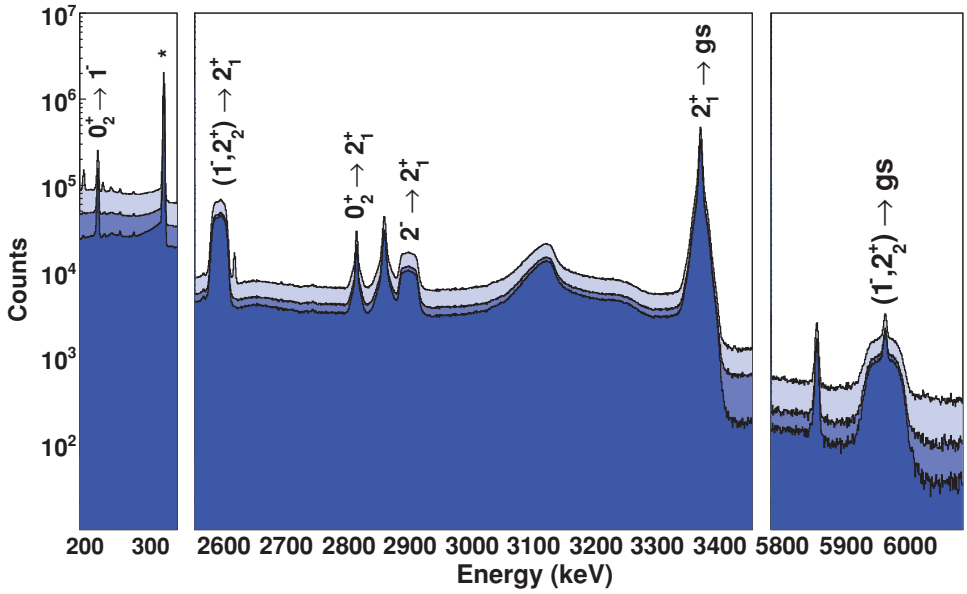

FIG. 1. (Color online) γ spectrum recorded following the β decay of ^{11}Li. Shown only are energy sections where ^{10,11}Be γ transitions are present. γ singles, β-γ, and bremsstrahlung-vetoed β-γ coincidences are displayed in increasingly darker shades of blue. The transition marked with a star (*) is the 320-keV $1/2^- \rightarrow 1/2^+$ transition in ^{11}Be. The other transitions belong to the decay of ^{10}Be excited states.

predictions that can be deduced experimentally from the measurement of excited state half-lives and branching ratios in ^{10}Be.

In recent years, three experiments [4–6] provided new information regarding the ^{11}Li β-delayed one-neutron emission, but a number of discrepancies remain, especially with respect to the identification of the delayed neutron branches. The latter experiment [6] is the only one that measured a delayed neutron spectrum. The other two [4,5] relied on the analysis of Doppler-broadened γ line shapes following the decay of ^{10}Be excited states to extract the energy of the neutrons involved in the decay. The line-shape analysis technique will be described in detail later, as it is also the basis of the work presented in this paper. Aside from the discrepancies that needed to be clarified (and will be discussed throughout this paper), the analysis from Ref. [6] shows that the complicated nature of the neutron energy spectrum is not yet fully understood, especially in the 1–2 MeV region. A new study was therefore warranted to resolve the existing discrepancies and clarify the interpretation of the neutron spectrum.

II. EXPERIMENTAL SETUP AND MEASUREMENT

The β decay of ^{11}Li was studied with the 20 Compton-suppressed high-purity germanium (HPGe) detectors comprising the 8π γ-ray spectrometer [13], with the added benefit of the enhanced ^{11}Li beam intensity available at TRIUMF and the addition of SCEPTAR, an inner array of 20 1.6-mm-thick plastic scintillators for β detection [14]. Each scintillating detector is collinear to one HPGe detector such that each γ-ray detector views the center of the array through only one scintillator. The ^{11}Li beam was produced by impinging a 500-MeV, 40-μA proton beam upon a 22.4-g/cm^2 tantalum target, and extracted via surface ionization into a beam of about 12000 atoms/s. The 30.6-keV ^{11}Li beam was transported to the center of the 8π spectrometer, where it was implanted in a thick (with respect to the implantation depth of the ions) aluminum foil. Data was collected independently from the 8π and the SCEPTAR arrays and pieced together using time-stamping, so that β-γ coincidences could be analyzed.

Data from the ^{11}Li β decay was collected for approximately 100 hours over a 2-week time period. About 5.0×10^7 β-γ coincidence events were collected during the experiment. Collinear plastic-HPGe coincidences were vetoed in order to reduce the contribution of bremsstrahlung radiation in the experimental γ-ray spectrum. Figure 1 shows energy sections of the γ spectrum, where γ-ray transitions in ^{10,11}Be are present. As can be seen, the signal-to-background ratio is clearly improved by using bremsstrahlung-vetoed β-γ events despite the loss of statistics. The Doppler-broadened nature of the observed γ line shapes will be discussed in detail in the next section. The γ spectrum does not reveal any previously unobserved γ-ray transitions.

The energy and intensity of the γ-ray transitions measured in this experiment are summarized in Table I and found to be in very good agreement with the results of the earlier experiment [5].

III. MONTE CARLO SIMULATION

The Doppler broadening of the ^{10}Be γ-ray line shapes result from the significant recoil induced by the neutron emission following the ^{11}Li β decay. Conservation of linear momentum implies that the kinetic energy of the recoil is about 1/10 that of one of the neutrons (which is typically of the order of 1–2 MeV; see the neutron energy spectrum in Hirayama *et al.* [6], for example). As the neutron emission is isotropic in the laboratory frame, so is the angular distribution of the recoil. It follows that the γ-ray angular distribution is also isotropic with respect to the laboratory frame, although there can be in some cases angular correlations between the neutron and the γ rays. The lifetime of the excited state populated also needs to be taken into account, as it defines the characteristic time period over which the recoil is allowed to slow down in the

TABLE I. Excited states in ^{10}Be and ^{11}Be. Energy (E_γ), intensity, and branching ratio (BR) of the γ transitions in ^{10}Be observed after the β-delayed neutron emission of ^{11}Li (unless noted). The intensities are normalized to the 3367-keV transition (100).

E_{level} (keV)	E_γ (keV)	Assignment	Intensity	BR(%)
320.04(1)	320.0(5)	^{11}Be: $\frac{1}{2}^- \rightarrow \frac{1}{2}^+$	23.1(12)	100
3368.03(3)	3367.1(5)	$2_1^+ \rightarrow 0_1^+$	100	100
5958.39(5)	2590.5(5)[a]	$2_2^+ \rightarrow 2_1^+$	25.1(18)[b]	91(5)[a]
	5957.4(5)[a]	$2_2^+ \rightarrow 0_1^+$	2.48(18)[b]	9(5)[b]
5961.8(5)[a]	2593.0(5)[a]	$1^- \rightarrow 2_1^+$	0.89(14)[b]	34(4)[c]
	5959.9(5)[a]	$1^- \rightarrow 0_1^+$	1.72(28)[b]	66(4)[c]
6180.3(5)	219.2(5)	$0_2^+ \rightarrow 1^-$	1.58(8)	34.3(12)
	2812.1(5)	$0_2^+ \rightarrow 2_1^+$	3.02(6)	65.7(12)
6265.1(5)	2896.6(5)	$2^- \rightarrow 2_1^+$	6.31(13)	100[d]

[a]Energies determined from fitting $(1^-, 2_2^+)$ doublet states.
[b]Intensities and branching ratios determined from fitting the $(1^-, 2_2^+)$ doublet states (see text).
[c]Determined from γ-γ coincidences and from fitting the $(1^-, 2_2^+)$ doublet states (see text).
[d]No evidence is found for other transitions from the 2^- state.

aluminum foil before it γ-decays. To first order, a short lifetime produces a Doppler-broadened rectangular line shape in which the whole range of Doppler shifts is essentially represented equally. A long lifetime on the other hand yields a sharper-looking peak induced by the slowing down effect of the recoil, but with a characteristic broad base, remnant of the original full Doppler broadening. Precise understanding of the line shapes and the extraction of quantitative information from line-shape analysis, however, require the development of detailed Monte Carlo simulations [4,5,15] taking into account a large number of parameters that can influence the line shapes. The following sections describe some of the main ingredients of the simulation used in the present work.

A. Implantation and geometric effects

With the implantation foil at the center of the 8π, one would expect that the experimental setup is symmetric with respect to the location of the implantation foil. However, because the typical initial energy of the recoil is of the order of a few hundred keV, much higher than the original beam implantation energy, some ^{10}Be ions can recoil back out of the foil. Depending on the lifetime of the ^{10}Be excited states, some γ rays can be emitted outside of the foil by recoils that are no longer slowing down. Experimentally, a signature of this effect is to observe more blue-shifted γ rays in the back ring of the 8π and more red-shifted γ rays in the front ring. Figure 2 shows that such an effect is indeed observed for the 2812-keV $0_2^+ \rightarrow 2_1^+$ transition because of the long-lived nature of the 0_2^+ state, but it does not occur for the 2897-keV $2^- \rightarrow 2_1^+$ transition pointing to a short-lived 2^- state. It is worth noting that it is not necessary to track down the recoils outside of the foil, as they do not travel significantly far from the foil before emitting their γ rays. This would have been different,

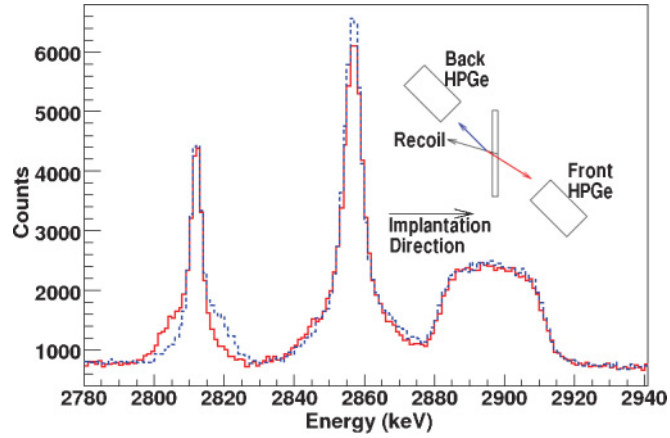

FIG. 2. (Color online) γ-ray spectrum recorded by the back (blue dashed line) and front (red solid line) HPGe rings of the 8π spectrometer. The excess of blue/red-shifted γ rays can be clearly seen in the 2812-keV transition and is absent in the 2897-keV transition. The central peak is the single-escape peak of the 3367-keV $2_1^+ \rightarrow 0_1^+$(g.s.) transition. Also shown is a schematic of the geometric asymmetry inducing the blue/red-shift excess effect.

of course, if much longer lived states were involved in the process.

The asymmetry observed in the data is accurately reproduced in the Monte Carlo by simulating the implantation depth profile of the ^{11}Li ions in the aluminum foil using the SRIM software [16] and considering the aluminum foil as infinitely thick in all directions, except for the direction upstream of the beam implantation. As the relative contributions of each HPGe ring potentially affect the overall line shape, the response of each ring was simulated individually and then combined with their relative γ efficiency.

B. Recoil due to the β-decay leptons

In most cases, the β decay induces a negligible contribution to the ^{10}Be recoil. However, in extreme circumstances (neutrino and electron emitted parallel to the direction of the neutron), the β decay can in principle contribute measurably to the maximum Doppler-broadening. The β-decay process was therefore included in the simulations as a precautionary measure. It was eventually shown that it has no visible impact on the line shape, simply because these extreme events only correspond to an extremely small fraction of the total possible momentum phase space.

C. Neutron emission

The neutron emission is simulated by drawing randomly a direction of emission with respect to the direction of implantation, while the energy of the neutron emitted is calculated based on the pair of ^{11}Be and ^{10}Be excited states it links. The width of the ^{11}Be neutron emitting state is taken into account by drawing the energy of the ^{11}Be state in a Breit-Wigner distribution of width Γ centered around energy E_0 (see Fig. 3). The Breit-Wigner distributions were truncated

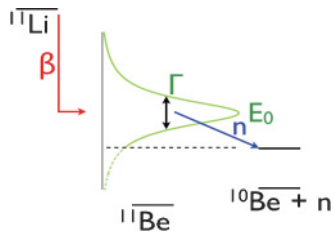

FIG. 3. (Color online) Schematic of neutron emission from an excited state in ^{11}Be. The state is modeled as a Breit-Wigner distribution (green solid line), with centroid E_0 and width Γ. The low-energy tail in the dotted line shows the part of the distribution truncated to forbid negative neutron energies.

below the energy, resulting in the emission of a neutron with no kinetic energy.

In principle, the energy E_0 and width Γ of each neutron-emitting state can be extracted from the line-shape analysis. In practice, however, only the known states in ^{11}Be, as well as a few unconfirmed ones, were considered as part of the search and are summarized in Table II. This was done in part to reduce the number of free parameters of the fit and to avoid the convergence to spurious states in the most complex line-shape analyses.

Broad states of the same spin and parity can interfere, constructively and destructively, with one another, if they are close enough in energy with respect to their combined width. Based on the recent spin assignments from Ref. [6] and the assumption that only previously observed ^{11}Be excited states contribute to the decay, we find that there could be an interference between the 8.03-MeV and the 8.82-MeV states. However, information is lacking with respect to the nature of the interference, so this potential effect was not included in the Monte Carlo simulations.

TABLE II. Excited states in ^{11}Be populated in the β decay of ^{11}Li and able to feed ^{10}Be excited states. Energy levels in *italics* are levels suggested but unconfirmed. Tentative assignments are shown in parentheses. Data are from Ref. [17] unless otherwise specified.

E_0 (MeV)	Γ (keV)	J^π	Ref.
3.887(15)	<10	$5/2^-$	
3.956(15)	15(5)	$3/2^-$	
5.240(21)	45(10)	$5/2^-$[a]	
5.61[b]	–	$(1/2^-,3/2^-)$	[18]
7.030(50)	300(100)	$5/2^-$	
8.03(2)	230(55)	$3/2^-$[a]	[3,6]
8.816(32)	200(50)	$3/2^-$[a]	
9.1[b]	–	$(3/2^-)$	[18]
10.0[b]	–	$(5/2^-)$	[18]
10.590(50)	210(40)	$5/2^-$[a]	
14.5(2)	*1100(200)*	–	[19]
18.15(15)	800(100)	–	[20]

[a]Spin-parity assignment from Ref. [6].
[b]Suggested to improve the fit of the neutron spectrum but does not appear in the following paper based on the same data [6].

D. Slowing down process

The slowing down process is central to the line-shape analysis, as the deduced lifetimes depend strongly on the rate of slowing down of the recoil in the foil [15]. From the initial recoil energy, the slowing down process is assessed every femtosecond using the stopping power estimated by the software SRIM. The SRIM stopping power in the region of interest compares well with the data available from Mertens and Krist [21], who measured the stopping power of beryllium ions in aluminum in the 90–300 keV energy range. The stopping powers estimated by SRIM depend on a number of adjusted parameters to achieve the best fit of all existing data. As a result, energy-dependent systematic errors need to be included for a given ion-target pair. Unfortunately, these are essentially impossible to estimate at most energies because of the lack of existing experimental data. This is especially true at very low energy, where slow recoils contribute to the line shape, whether they arise from low-energy neutron feedings or because of the long lifetime of the excited state. A comparison of energy loss models in the context of the Doppler-broadened line-shape analysis is discussed in Ref. [15]. In what follows, we assigned an energy-independent systematic error of ±10% to the SRIM stopping powers used in the simulation. The error propagation to the extracted parameters of the fit was assessed by repeating each line-shape analysis with stopping powers changed by ±10%. Aside from the lifetime of the excited state considered, the other parameters of the fit are found to be essentially insensitive to the variations in stopping power.

E. γ decay and intrinsic HPGe line shape

For nonzero angular momentum ℓ carried away by the neutron and nonzero J spin of the excited states in ^{10}Be, neutron-γ angular correlations can affect the γ line shape of a transition. Particle-γ angular correlations are discussed in the classic paper by Biedenharn and Rose [22], from which one can extract the range of possible angular correlations based on the possible channel spins. Once the calculations are carried out, the angular correlation is expressed by a sum of Legendre polynomial $P_\nu(\cos\theta)$, with the significant term given by $\nu = 2$ and the associated factor A_2 defining both the sign and the strength of the correlation. In most cases, the theoretical determination of the A_2 coefficients is not possible, because the relative contributions of each channel spin connecting the neutron-emitting state to the γ-emitting state are not known. This can be rendered even more difficult in the case of mixed M_L/E_{L+1} electromagnetic transitions, where the correlation also depends on the ratio of the reduced matrix elements, which are not always known [22]. As a result, only a range for the A_2 parameters can be estimated, hence the A_2 parameters need to be included as free parameters. This poses a serious difficulty in the analysis, as the lifetimes extracted from the line-shape analyses are found to be strongly correlated with the A_2 coefficients [5,15]. Angular correlations will be discussed further in the line-shape analysis of the $(1^-, 2_2^+)$ doublet.

Another ingredient of the Monte Carlo simulation is to take into account the response of the HPGe detectors by modeling accurately the intrinsic line shape of a γ peak not subjected to

TABLE III. γ-ray transitions in ^{11}B following the β decay of ^{11}Be used in the HPGe energy and efficiency calibrations. Energies given in keV. From Ref. [24].

E_{level}	J^{π}	E_{γ}	Intensity
2124.69(3)	$1/2^{-}$	2124.47(3)	100
6791.8(3)	$1/2^{+}$	4665.9(4)	5.12(14)
		6789.8(5)	12.62(62)
7977.8(4)	$3/2^{+}$	5851.5(4)	6.01(24)
		7974.7	5.34(40)

any Doppler broadening. For this, we use a fitting formula also used in the GF3 routine of the RADWARE software package [23] and given below in Eq. (1).

$$F(x) = c_1 \frac{1}{\sigma\sqrt{2\pi}} e^{-(x-\mu)^2/2\sigma^2} + c_2 e^{[(x-\mu)/\beta+\sigma^2/2\beta^2]} \text{erfc}\left(\frac{x-\mu}{\sqrt{2}\sigma} + \frac{\sigma}{\sqrt{2}\beta}\right) + c_3 \text{erfc}\left(\frac{x-\mu}{\sqrt{2}\sigma}\right). \quad (1)$$

The fitting formula consists of the usual Gaussian distribution and also includes a skewed Gaussian modeling the incomplete charge collection and another term modeling the background, including the multiple Compton scattering contribution on the low energy side of the peak. The free parameters of the fit, such as the resolution σ and the skew factor β, are adjusted as a function of the energy by fitting non-Doppler-broadened transitions observed in the spectrum. Of particular interest are the transitions in ^{11}B following the β decay of ^{11}Be also present in the spectrum and given in Table III. These transitions are ideal benchmarks for adjusting the fit parameters in the energy range where the Doppler-broadened line shapes are found. As an example, Fig. 4 shows the fit performed on the 6790-keV transition in ^{11}B.

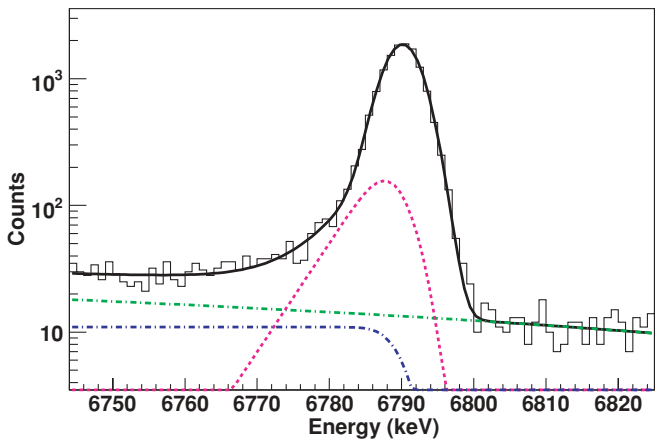

FIG. 4. (Color online) Fit of the 6790-keV transition in ^{11}B using Eq. (1) plus an additional linear background. The components of the fit are shown in dashed lines of different colors.

F. Fitting algorithm and error analysis

A χ^2 method is used to test the validity of our model in reproducing effectively the experimental line shapes. The Doppler-broadened line shapes recorded in the ^{11}Li decay depend on a potentially large number of free parameters, and so a robust fitting procedure is needed to search through the parameter phase space. The Levenberg-Marquardt algorithm was used to search for the best value of all parameters simultaneously. Levenberg-Marquardt is an iterative maximum-likelihood estimator [25] in which an initial guess for the parameters and uncertainties is repeatedly updated until a convergence condition is reached. The algorithm is computationally intensive: at each iteration, partial derivatives with respect to each free parameter must be evaluated numerically, requiring a total of $2N + 1$ simulations per step (N is the number of free parameters). The covariance matrix between free parameters is calculated at each step, along with the χ^2, and an updated guess for the parameters is deduced. A numerical method for implementing the Levenberg-Marquardt algorithm can be found in Ref. [26].

Because of the high statistics collected in the experimental line shapes, a large number of events need to be simulated so that statistical uncertainties in the simulations can be considered negligible. To reduce the time required to perform these simulations, the simulations have been performed in parallel on a local network using a custom client/server software written at the Colorado School of Mines. Due to the limited availability of the computers used on the network, the number of free parameters (which determines the total number of simulations to be performed) needed to be reduced when possible. This was done in particular for the values of energy centroids, since they are found to lie in very deep χ^2 wells and are not correlated to other parameters.

Once the final iteration of the Levenberg-Marquardt algorithm is performed, the final error matrix is produced with the diagonal elements providing the uncertainties for each free parameter included in the fit. A χ^2 of the best fit is computed from which the reduced χ^2/ν can be deduced knowing the number of degrees of freedom ν. In the algorithm, the uncertainties on the free parameters are given based on the assumption that the fit is successful, i.e., $\chi^2/\nu \approx 1$. The uncertainties must therefore be increased in the cases where χ^2/ν is significantly greater than 1. To estimate the final error bars on the measurements, the uncertainties deduced from the algorithm were weighted by $\sqrt{\chi^2/\nu}$, as suggested in Ref. [27].

IV. RESULTS

In this section, we present the results of the line-shape analyses performed for each Doppler-broadened transition observed in the γ spectrum. As we need to take into account potential indirect feedings from higher excited states, we discuss the analysis starting from the highest excited state in ^{10}Be and make our way down the ^{10}Be decay scheme.

A. The $2^{-} \rightarrow 2_1^{+}$ transition

The original analysis performed in Ref. [5] suggests that the γ line shape can be understood by considering a single neutron

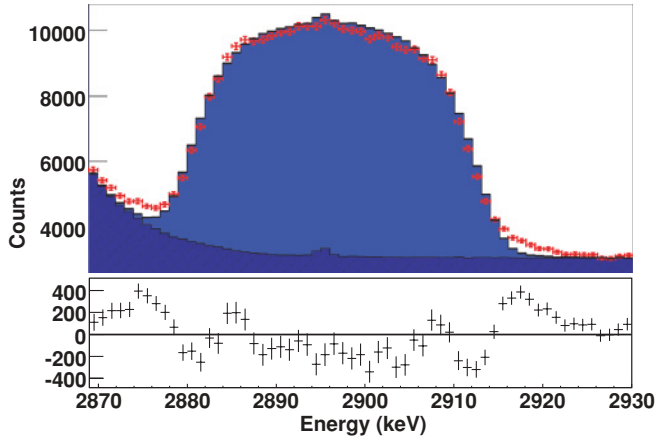

FIG. 5. (Color online) Line-shape analysis of the 2897-keV $2^- \rightarrow 2_1^+$ transition using only the 8.82-MeV neutron-emitting state in ^{11}Be. The difference between the experimental data and the simulation is shown below the figure.

feeding from the 8.82-MeV state in ^{11}Be and a 2^- half-life of 85 ± 12 fs (stat + syst). To investigate the 2897-keV line shape in the new experiment, the background below the peak was first estimated. This consisted of generating the high-energy tail of the single-escape peak of the 3367-keV transition and adding the known weak contribution at 2895.3 keV resulting from the β decay of ^{11}Be to the 5020-keV state in ^{11}B to a linear background normalized to the high-energy side of the γ line shape. A fit, using the same neutron feeding as originally suggested, was then performed on the new γ line shape and is shown in Fig. 5. A poor reduced χ^2/ν of the order of 3.8 is found. The residual (difference between the data and the simulation) spectrum, plotted below the fit, clearly shows areas of discrepancies, hinting in particular at a new contribution from a higher energy branch not previously reported. Discrepancies are also observed in intermediate sections of the line shape.

Through an iterative process and by considering the features of the residual at each step, it was possible to find the energy of the contributing states in ^{11}Be. Starting from the 8.82-MeV single branch feeding, the fit was repeated by successively adding contributions from the 8.03-, 10.6-, and 7.03-MeV states, which resulted in a significant decrease of the χ^2 estimate. Table IV shows the evolutions of the χ^2 and the associated p value, which describes the probability that a random sample of data points taken from the true probability distribution would yield a value of χ^2 as large as or larger than the one obtained in the best fit proposed for each model considered.

The best fit ($\chi^2/\nu = 1.244$, $\nu = 75$) is found to require four different neutron branches originating from the 7.03-, 8.03-, 8.82-, and 10.6-MeV states (see Fig. 6). Since all these states are known to be either $3/2^-$ or $5/2^-$, the feeding of the 2^- state is done most likely by $\ell = 0$ neutrons, hence the γ decay is not subjected to any n-γ correlations. Taking into account the new branches, the half-life of the 2^- state is found to be 3.2(24) fs (statistical error only), considerably smaller than previously thought. With such a short half-life, the influence of the stopping powers is mostly negligible, and the overall line

TABLE IV. Evolution of the χ^2 ($\nu = 75$) and of the associated p value obtained when fitting the $2^- \rightarrow 2_1^+$ line shape with an increasing number of neutron branches. As can be seen, the added contribution of all four branches is needed to best describe the experimental line shape. The evolution of the 2^- half-life is also given for information.

Branches (MeV)	χ^2	p value	$T_{1/2}$ (fs)
8.82	285.0	~0	79.1
+8.03	265.5	~0	40.5
+10.6	120.7	0.0006	15.8
+7.03	93.3	0.0748	3.2

shape becomes much more sensitive to the other parameters, such as the width of the contributing ^{11}Be states, which are not known with very good precision. In this context, an upper limit on the 2^- half-life is more appropriate to account for the uncertainties on all the parameters included in the fit. Taking into account a deviation of about 2σ from the deduced value, we suggest an upper limit for the new 2^- half-life of 8 fs.

Table V summarizes the contributions of each individual branch and also includes the energy of the neutron emitted and the maximum Doppler shift induced by the neutron emission from their respective excited states in ^{11}Be. As a consistency check, we look at the neutron energy spectrum recorded in Ref. [6]. According to our analysis, about 2/3 of the intensity making up branch 11 in Ref. [6] should in fact be located in the 1.14-MeV region, where the neutron spectrum is actually poorly understood. We note that a change in the β-asymmetry pattern occurs for neutrons in the 1.1-MeV region, suggesting the presence of a previously unaccounted for neutron branch most likely arising from a $3/2^-$ state in ^{11}Be, which is precisely the case of the 8.03-MeV state. The two other neutron branches, originating from the 7.03- and 10.6-MeV states in ^{11}Be, are too weak to have observable contributions in the neutron energy spectrum, although they could change slightly the intensity of all the surrounding branches contributing to the spectrum.

The new lifetime extracted from this experiment yields a lower limit on the $B(E1; 2^- \rightarrow 2_1^+)$ of 7.5×10^{-3} W.u.

TABLE V. Line-shape analysis of the $2^- \rightarrow 2_1^+$ 2897-keV transition. The intensity breakdown is given for each contributing neutron-emitting state in ^{11}Be together with the energy of the emitted neutrons E_n and the maximum Doppler shift (ΔE_{max}) it induces in the transition considered.

$J^\pi = 2^-$	$T_{1/2} < 8$ fs (syst. error negligible)		
From ^{11}Be			
E_{level} (MeV)	E_n (MeV)	ΔE_{max} (keV)	Intensity
7.03	0.24	6.55	0.15(3)
8.03	1.15	14.41	4.01(15)
8.82	1.86	18.38	1.75(14)
10.6	3.48	25.11	0.40(5)
Total			6.31(13)

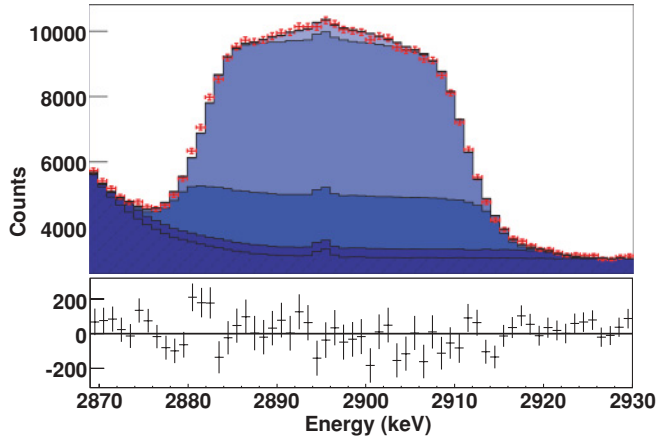

FIG. 6. (Color online) Line-shape analysis of the 2897-keV $2^- \rightarrow 2_1^+$ transition. The best fit is obtained using the parameters given in Table V. The relative contribution of each neutron branch is shown by using different shades of blue. The difference between the experimental data and the simulation is shown below the figure.

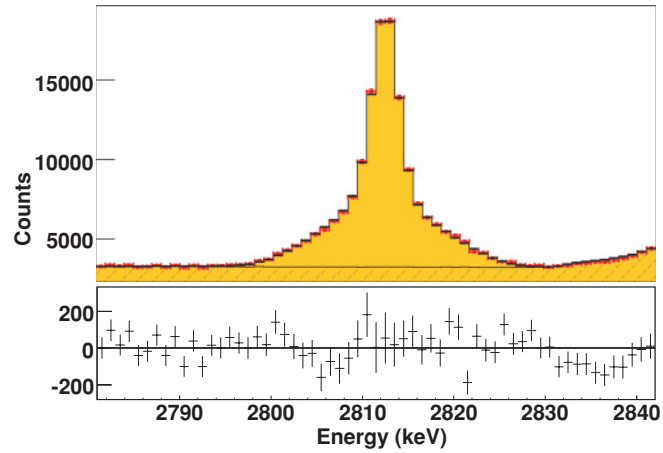

FIG. 7. (Color online) Line-shape analysis of the 2812-keV $0_2^+ \rightarrow 2_1^+$ transition. The best fit is obtained using the parameters given in Table VI. The difference between the experimental data and the simulation is shown below the figure.

using the 8-fs half-life upper limit (0.018 W.u. when using the nominal value of 3.2 fs) extracted from the best fit, about 10 times higher than the previous value of 7.7×10^{-4} W.u. proposed in Ref. [5]. This new value is now within range of the most recent theoretical works using the no-core shell model (NCSM, 0.022 W.u.) and four-body microscopic cluster model (MCM, 0.02 W.u.) approaches, which interpret the 2^- state in ^{10}Be as an excited one-neutron halo state [10]. This measurement also confirms the existence of a decay pathway linking the 8.82-MeV state in ^{11}Be to the 2^- state in ^{10}Be. The nature of the 8.82-MeV state will be discussed further following the line-shape analyses arising from the decay of the $(1^-, 2_2^+)$ doublet states.

B. The $0_2^+ \rightarrow 2_1^+$ transition

The line-shape analysis of the 2812-keV transition is shown to arise from the feeding of a single neutron branch arising from the 8.03-MeV state in ^{11}Be, as previously suggested in Ref. [5]. The best fit ($\chi^2/\nu = 1.240$, $\nu = 56$) is shown in Fig. 7 and the contributing branch parameters displayed in Table VI. No n-γ angular correlation is expected in this case, since the γ rays emitted from a 0^+ state are isotropic by nature. The half-life extracted from the fit is found to be 983(27) fs (statistical error only), in reasonable agreement with the previous half-life of 870(70) fs deduced from Ref. [5]. The discrepancy between the two measurements indicates another potential limitation of the method when considering long half-life. As the half-life gets longer and longer, the changes of the line shape become more subtle, resulting in a relative loss of sensitivity.

Figure 8 shows the evolution of the recoiling ^{10}Be energy [Fig. 8(a)] and of the Doppler-broadening [Fig. 8(b)] of the 2812-keV line shape as a function of time as estimated in the Monte Carlo simulation. As can be seen, the characteristic time to stop a ~100-keV ^{10}Be recoil making up most of the recoils is on the order of 800 fs. Beyond this time, only a small fraction of events in the high-energy tail of the Breit-Wigner distribution still generates significant Doppler

TABLE VI. Line-shape analysis of the $0_2^+ \rightarrow 2_1^+$ 2812-keV transition. The intensity is given for the contributing neutron-emitting state in ^{11}Be together with the energy of the emitted neutrons (E_n) and the maximum Doppler-shift ($\Delta E_{\max}$) it induces in the transition considered.

$J^\pi = 0_2^+$	$T_{1/2} = 983 \pm 27$ (stat.)$^{+200}_{-120}$(syst.) fs		
From ^{11}Be			
E_{level} (MeV)	E_n (MeV)	$\Delta E_{\max}$ (keV)	Intensity
8.03	1.22	14.45	3.02(6)
Total			3.02(6)

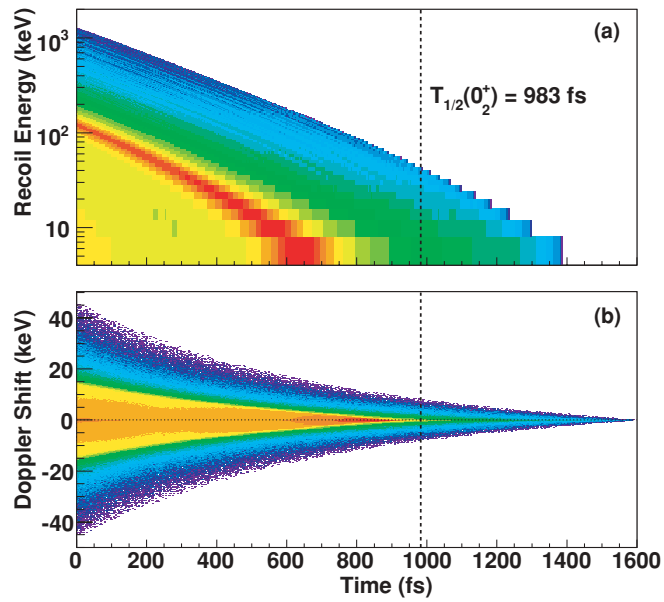

FIG. 8. (Color online) (a) Evolution of the ^{10}Be recoil energy as a function of time after the neutron emission ($t = 0$). (b) Evolution of the Doppler broadening as a function of the same time.

broadening. The "sharp" component of the line shape therefore becomes less and less sensitive to the Doppler-broadening process as the half-life of the excited state increases and becomes more sensitive to the intrinsic response of the HPGe. A slight change of the HPGe parameters used in the two analyses then may be responsible for the discrepancies observed. Another illustration of this effect is obtained when considering a model also including a low-energy neutron branch from the 7.03 MeV state in ^{11}Be. In this case, a best fit with a slightly better χ^2 is obtained with a contribution of up to 5% of the total intensity from the 7.03-MeV branch and a 0_2^+ half-life of about 900 fs. Such a small contribution in the same range of energy where the intrinsic HPGe resolution is known to possibly affect the line shape may turn out to be spurious for the reason given above. As a consequence, this potential additional branch is not considered in the final result.

The dominant source of error remains the systematic error due to the uncertainty on the energy loss. A systematic ±10% change in the stopping powers used in the simulation results in a shift of $^{+200}_{-120}$fs, respectively, of the deduced half-life, hence the half-life given in Table VI. At the end, the half-lives deduced by including or not including a 7.03-MeV contribution are consistent within the total error bar given.

The second 0_2^+ in ^{10}Be was recently identified as a molecular rotation bandhead [28] with a cluster structure in which two valence neutrons induce an increase of distance between the two α particles [29]. In this context, the long 0_2^+ half-life is explained by the significant difference of structure between this state and the two first states of ^{10}Be. The $B(E1; 0_2^+ \rightarrow 2_1^+)$ of 4.8×10^{-2} W.u. extracted from the new experimental half-life is in good agreement with the one obtained from antisymmetrized molecular dynamics calculations (2.0×10^{-2} W.u.) suggesting the clustered nature of the 0_2^+ state [29].

C. The $(1^-, 2_2^+) \rightarrow 2_1^+$ and $(1^-, 2_2^+) \rightarrow 0_1^+$ transitions

The line shapes of the transitions from the $(1^-, 2_2^+)$ doublet to the first 2^+ state and to the ground state need to be analyzed together to account for the relative intensities of each individual direct or indirect contribution. By gating on the $0_2^+ \rightarrow 1^-$ transition, the intensities and line shapes of the $1^- \rightarrow 2_1^+$ and $1^- \rightarrow 0_1^+$ transitions are extracted. The branching ratio of the 1^- state to the first 2^+ state in ^{10}Be is found to be 34(4)%, consistent with the value suggested in Ref. [5]. The best fit ($\chi^2/\nu = 0.447$, $\nu = 226$) of the two line shapes analyzed together (see Figs. 9 and 10) yields a 44(40)-fs half-life for the 1^- state in ^{10}Be and confirms the feeding of the 0_2^+ state from the 8.03-MeV ^{11}Be state. The poor resolution on the lifetime measurement is explained by the fact that the line shape is mostly due to the long 0_2^+ half-life and is not as sensitive to the much shorter 1^- half-life. The 1^- half-life is found to be significantly lower than the one suggested by Fynbo *et al.* [4].

Following this preliminary step, the line shapes induced by the decay of the doublet are investigated. At least two ^{209}Bi$(n, n'\gamma)\gamma$ lines are found to contaminate the $(1^-, 2_2^+) \rightarrow 2_1^+$ line shape and are included in the background. Other

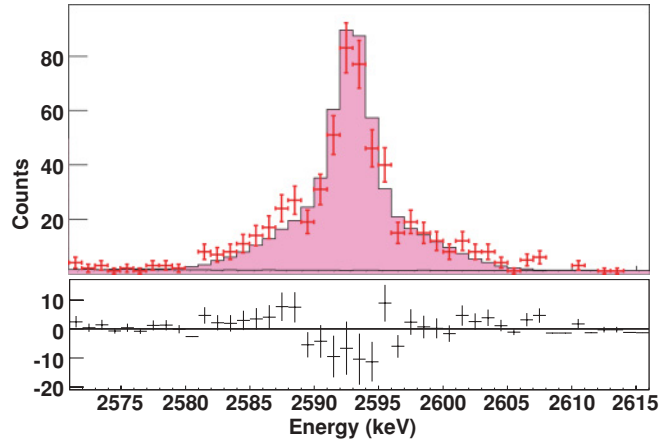

FIG. 9. (Color online) Line-shape analysis of the $1^- \rightarrow 2_1^+$ transition isolated by gating on the $0_2^+ \rightarrow 1^-$ transition. The difference between the experimental data and the simulation is shown below the figure.

$(n, n'\gamma)$ reactions can potentially contribute more weak lines in the energy range of interest, but their relative intensities could not be ascertained. The decision was thus made not to include them in order to avoid biasing the data. A look at the intensities feeding and originating from the doublet indicates that about 95% of all the intensity comes from direct feeding of the doublet. In the two previous studies analyzing the line shapes arising from the doublet decay [5,15], two features are identified: a broad base due to the direct feeding of the 2_2^+ state (and possibly of the 1^- state as well) and a sharp component resulting from the decay of the long-lived 0_2^+ state to the 1^- state. The relative dominance of the former in the $(1^-, 2_2^+) \rightarrow 2_1^+$ line shape points to a large $2_2^+ \rightarrow 2_1^+$ branching ratio, consistent with existing data in the literature [17]. Direct feeding of the 2_2^+ requires the emission of odd ℓ neutrons, calling for the need to include neutron-γ correlations. To narrow down the contributing neutron branches, the line-shape analysis was performed first without including angular correlations.

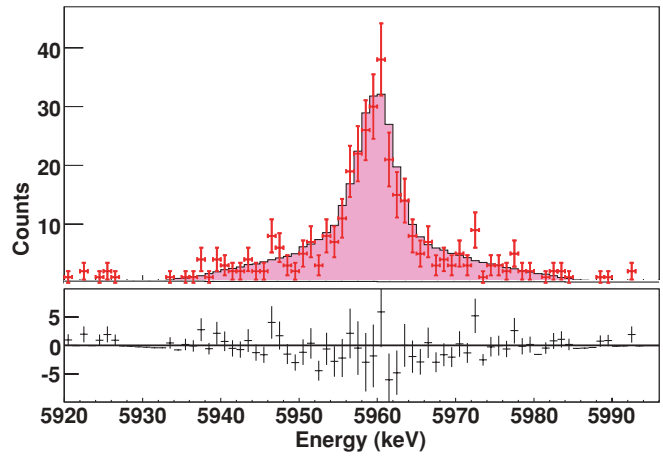

FIG. 10. (Color online) Same as Fig. 9, but for the $1^- \rightarrow 0_1^+$ transition isolated by gating on the $0_2^+ \rightarrow 1^-$ transition.

Discrepancies exist regarding the neutron feeding of the 2_2^+ state: Sarazin *et al.* suggest that it is populated from the 8.03- and 8.82-MeV states in ^{11}Be [5], while Hirayama *et al.* only find evidence of the 8.03-MeV feeding [6]. A very poor fit ($\chi^2/\nu \sim 15$) is obtained in this work when only considering the indirect feeding of the 1^- state from the 0_2^+ state and the direct feeding of the 2_2^+ state from the 8.03-MeV state in ^{11}Be. The best fit ($\chi^2/\nu = 2.308$, $\nu = 251$) is found by including the disputed contribution from the 8.82-MeV state in ^{11}Be (albeit with a lower intensity than previously suggested) and two other weak contributions directly feeding the 1^- state. The two latter contributions are essentially added to improve the $(1^-, 2_2^+) \rightarrow 0_1^+$ line shape, but have a negligible impact on the $(1^-, 2_2^+) \rightarrow 2_1^+$ line shape because of the combination of relative feeding and branching ratios of the 1^- and 2_2^+ states. As a consequence, the deduced 2_2^+ half-life, which is primarily obtained from the fit of the $(1^-, 2_2^+) \rightarrow 2_1^+$ line shape, remains the same independent of the existence of these two weak contributions. The half-life of the 2_2^+ state is found to be 61.4(2) fs (statistical only) in excellent agreement with Ref. [5]. The fit of the $(1^-, 2_2^+) \rightarrow 2_1^+$ and $(1^-, 2_2^+) \rightarrow 0_1^+$ line shapes are shown in Figs. 11 and 12, respectively. The residuals in Fig. 11 still show an apparent systematic behavior that could indicate the existence of more unidentified direct feedings. It is also possible that the residual points indirectly to the existence of other unaccounted for contaminating γ lines, from $(n, n'\gamma)$ reactions, for example.

Next, the line-shape analysis is repeated taking into account angular correlations. Only the decays proceeding through the 2_2^+ state may display n-γ correlations. From the previous analysis, this state is populated directly by the 8.03- and 8.82-MeV states in ^{11}Be, both believed to be $J^\pi = 3/2^-$ [6], and decays to the 2_1^+ and the 0_1^+(g.s.) states. In total, four A_2 angular correlation coefficients therefore need to be determined. Following the formalism described in Ref. [22], the range for each of the A_2 coefficients are determined. Considering

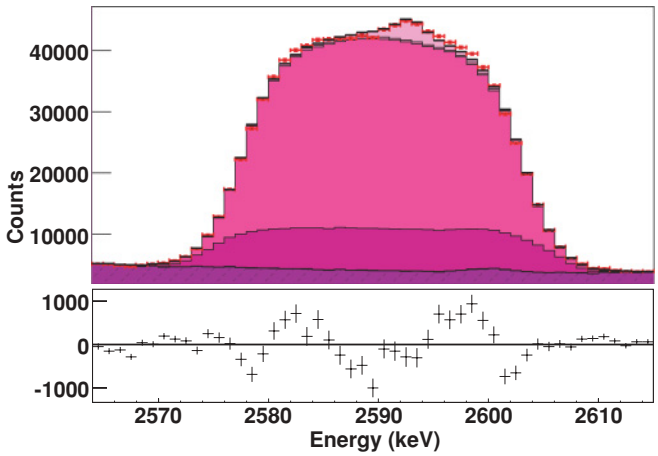

FIG. 11. (Color online) Line-shape analysis of the $(1^-, 2_2^+) \rightarrow 2_1^+$ doublet transition without n-γ correlations. The best fit is obtained using the parameters given in Tables VIII and VII. The relative contribution of each contributing branch is shown by using different shades of purple. The difference between the experimental data and the simulation is shown below the figure.

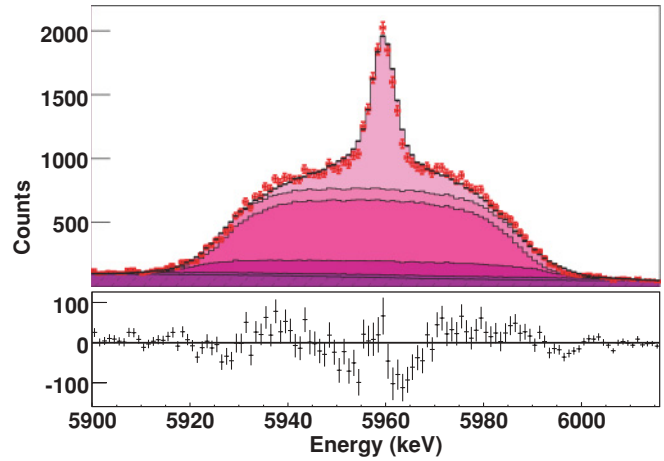

FIG. 12. (Color online) Same as Fig. 11, but for the $(1^-, 2_2^+) \rightarrow 0_1^+$ doublet transition without n-γ correlations.

a pure $E2\,2_2^+ \rightarrow 0_1^+$(gs) transition, the A_2 coefficients can be determined for each possible channel spin ($A_2 = -0.107$ for $s = 1$, and $A_2 = 0.107$ for $s = 2$). Unfortunately, because the relative contribution of each channel spin to the feeding is not known, only a range of possible A_2 values ($[-0.107,\ 0.107]$) can be deduced. The calculation is further complicated when considering the likely mixed $M1/E2\,2_2^+ \rightarrow 2_1^+$ transition. In this case, the correlation not only depends on the relative contribution of each channel spin, but also on the reduced matrix elements describing the admixture. Considering δ^2, the ratio of the $E2/M1$ squared matrix elements, the A_2 coefficient for a given channel spin can be expressed as a function of δ and is shown in Fig. 13.

When $\delta = 0$, the correlation is the one of a pure $M1$ transition and the A_2 coefficient is found to be $A_2 = 0.350$ (-0.350) for the $s = 1$ ($s = 2$) channel spin. When $|\delta| \gg 1$, the correlation converges to the one of a pure $E2$ transition as in the case of the $2_2^+ \rightarrow 0_1^+$(g.s.) transition. The existence

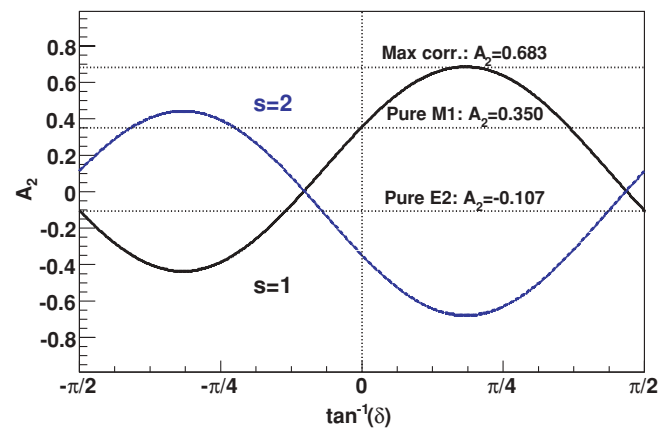

FIG. 13. (Color online) Neutron-γ correlation as a function of the $M1/E2$ admixture (δ) for channel spins $s = 1$ (black solid line) and $s = 2$ (blue dotted line). The x axis is expressed as $\tan^{-1}(\delta)$ to show the pure $E2$ case ($|\delta| \rightarrow \infty$). The significant A_2 values for channel spin $s = 1$ are highlighted (see text).

of an interference term in the correlation results in significant changes of the correlation between these two extreme cases. The maximum correlation is found for $\delta \approx 0.649$ [$\tan^{-1}(\delta) = 0.576$] with $A_2 = \pm 0.683$ depending on the channel spin considered (see Fig. 13). As in the previous case, because the relative contribution of each channel spin is unknown, one can only narrow down the A_2 coefficients associated with the $2_2^+ \rightarrow 2_1^+$ transition to within the $[-0.683,\ 0.683]$ range.

Line-shape analyses performed with all four A_2 coefficients added as free parameters reveal slight changes in the best fit parameters without significantly improving the quality of the fit. However, it is also found that the final A_2 values are strongly dependent on the original seed values, whereas all the other parameters (including the half-life) converge to very similar values. To estimate the maximum impact of the correlations on the half-life without attempting to measure them, two sets of simulation were performed where all A_2 parameters were simultaneously set to either their maximum positive or negative values. The 2_2^+ half-life is found to change by less than 2 fs when including the correlations, leading to a final value of 61.4(17) fs (stat). The relative contributions of all the branches feeding the 1^- and 2_2^+ states are given in Tables VII and VIII, respectively. The uncertainties given for the intensities also include the propagated uncertainties estimated from the correlations.

The present analysis suggests that the 8.82-MeV state in ^{11}Be is needed to account for the line shape of both transitions originating from the doublet. Its relative intensity with respect to the 8.03-MeV feeding remains in conflict with the coincidence data showed in the paper by Hirayama *et al.* [6], although one could argue that it is within the statistical uncertainties. Another possibility that cannot be excluded is the presence of other unknown contributing neutron branches that could reduce the relative intensity of the 8.82-MeV branch. Even in this case, because the full Doppler broadening of the line shapes is so well accounted for by the addition of the 8.82-MeV neutron branch, it is very unlikely that this branch does not contribute to the ^{11}Li decay scheme.

The 8.82-MeV state in ^{11}Be may play a pivotal role in the "halo survival" scenario suggested in the Introduction. Circumstantial evidence (see Ref. [5] and references therein, and Ref. [12]) exists indicating that the 8.82-MeV state can be understood as a $^9\mathrm{Be} + n + n$ configuration, possibly in a hybrid halo/cluster configuration. This may be formed when the β decay is occurring in the ^{11}Li core, leaving intact the neutron halo wave function. Interestingly, this state is found to decay to the 2_2^+, 1^-, and 2^- excited states, all three believed to be built upon a ^{9}Be core with a neutron either in an s-wave (1^-, 2^-) or in a p-wave (2_2^+) [10,30]. The excited halo nature of the 2^- state strongly suggests that the decay path from the 8.82-MeV state to the 2^- results from the emission of one of the s-wave halo neutrons. A similar argument can be made for the 1^- state which is suggested to be similar to the 2^- [31], although it is not necessarily expected that the 1^- state is itself an excited halo state, as it is farther away from the $^9\mathrm{Be} + n$ threshold. The experimental $B(E1; 1^- \rightarrow 2_1^+)$ and $B(E1; 1^- \rightarrow 0_1^+)$ are found to be in the range of 3.4×10^{-4} to 8.3×10^{-3} and 5.4×10^{-5} to 1.1×10^{-3} W.u., respectively. These values are lower than the values predicted from NCSM (2.7×10^{-2} W.u. [32]) for the former, and from a molecular orbit model (7.9×10^{-3} W.u. [33]) for the latter. Because of the large range of experimental $B(E1)$ values obtained, it is not reasonable to provide any kind of conclusive interpretation. A new independent experimental determination of the 1^- lifetime is desirable, as the present method has a known large inherent uncertainty due to the influence of the long 0_2^+ lifetime in the measurement.

TABLE VII. Line-shape analysis of the $1^- \rightarrow 2_1^+$ 2593-keV and $1^- \rightarrow 0_1^+$ 5960-keV transitions. In addition to the direct feeding from ^{11}Be neutron emitting states (see Table V for an explanation of the data displayed), the indirect feeding from excited states in ^{10}Be are also displayed. In this case, the energy of the contributing level, its spin-parity, branching ratio (BR) to the state of interest, and intensity are also indicated.

$J^\pi = 1^-$	$T_{1/2} = 44(40)$ fs (syst. error negligible)		
	$1^- \rightarrow 2_1^+$ transition:		
From ^{11}Be			
E_{level} (MeV)	E_n (MeV)	ΔE_{max} (keV)	Intensity
8.82	2.14	17.62	0.25(9)
10.6	3.76	23.35	0.10(3)
From ^{10}Be			
E_{level}(keV)	J^π	BR(%)	
6180.3(5)	0_2^+	34.3(12)	0.54(7)
Total			0.89(14)
	$1^- \rightarrow 0_1^+$ transition:		
From ^{11}Be			
E_{level} (MeV)	E_n (MeV)	ΔE_{max} (keV)	Intensity
8.82	2.14	40.51	0.49(18)
10.6	3.76	53.68	0.19(6)
From ^{10}Be			
E_{level}(keV)	J^π	BR(%)	
6180.3(5)	0_2^+	34.3(12)	1.04(13)
Total			1.72(28)

TABLE VIII. Line-shape analysis of the $2_2^+ \rightarrow 2_1^+$ 2590-keV and $2_2^+ \rightarrow 0_1^+$ 5957-keV transitions (see Table V for an explanation of the data displayed.)

$J^\pi = 2_2^+$	$T_{1/2} = 61.4 \pm 1.7(\mathrm{stat.})^{+7.8}_{-6.0}(\mathrm{syst.})$ fs		
	$2_2^+ \rightarrow 2_1^+$ transition:		
From ^{11}Be			
E_{level} (MeV)	E_n (MeV)	ΔE_{max} (keV)	Intensity
8.03	1.42	14.37	19.6(14)
8.82	2.14	17.62	5.5(8)
Total			25.1(18)
	$2_2^+ \rightarrow 0_1^+$ transition:		
From ^{11}Be			
E_{level} (MeV)	E_n (MeV)	ΔE_{max} (keV)	Intensity
8.03	1.42	33.04	1.94(14)
8.82	2.14	40.52	0.54(8)
Total			2.48(18)

The ^{11}Li halo is known to be an admixture of s- and p-wave neutrons [34], so one in principle expects that evidence for the emission of the p-wave halo neutron may also be present experimentally. The feeding of the 2_2^+ state from the 8.82-MeV state may just be this evidence if the configuration of the 2_2^+ state is indeed $^9\mathrm{Be} \otimes \nu_{p_{1/2}}$ as suggested by Arai [30]. The experimental $B(E2; 2_2^+ \rightarrow 0_1^+)$ value of 0.086 W.u. is well reproduced by NCSM and MCM calculations [10,35] adding confidence to these models. The experimental $B(E2; 2_2^+ \rightarrow 2_1^+)$ is found to be extremely large (56.1 W.u.), suggesting that the transition is at the very least a mixed $M1/E2$ transition and possibly a nearly pure $M1$ transition. A pure $B(M1)$ transition would lead to an experimental value of 0.02 W.u. in very good agreement with the $B(M1)$ of 0.03 W.u. predicted by NCSM [32].

D. The $2_1^+ \rightarrow 0_1^+$ transition

The 3367-keV line shape is extremely complex because of the contribution of a large number of direct and indirect branches, and it leads to an explosion of free parameters that cannot be handled by our Monte Carlo. To reduce the number of free parameters, the angular correlation parameters are all fixed to zero, and the allowed direct branches feeding the 2_1^+ state are limited to the ones suggested by Hirayama *et al.* Moreover, the 2_1^+ half-life used [$T_{1/2} = 142 \pm 3(\mathrm{stat.}) \pm 7(\mathrm{syst.})$ fs] is the one obtained by a recent DSAM experiment performed at Argonne National Laboratory [36]. In these particular conditions, the best fit remains very poor ($\chi^2/\nu = 21.7$, $\nu = 95$) but provides a good qualitative description of the experimental data, as seen in Fig. 14.

Relative contributions are given in Table IX, and they agree reasonably well with the analysis done by Ref. [6]. In particular, they confirm the existence of the neutron branches originating from the high-lying excited states in ^{11}Be. A very significant discrepancy is, however, observed for the intensities of the two lowest energy neutron branches compared to Ref. [6]. In this analysis, we find that the relative contribution of the 3.96-MeV state in ^{11}Be needs to be much larger than the one from the 3.89-MeV state to account for the line shape of the central section of the peak. Assuming this may possibly be due to an incorrect assessment of the intrinsic resolution and line shape of the HPGe around 3 MeV, where no strong calibration line exists, the analysis was repeated for reasonable values of the resolution. In all cases, we fail to reproduce the 3.96-MeV/3.89-MeV intensity ratio found in Ref. [6].

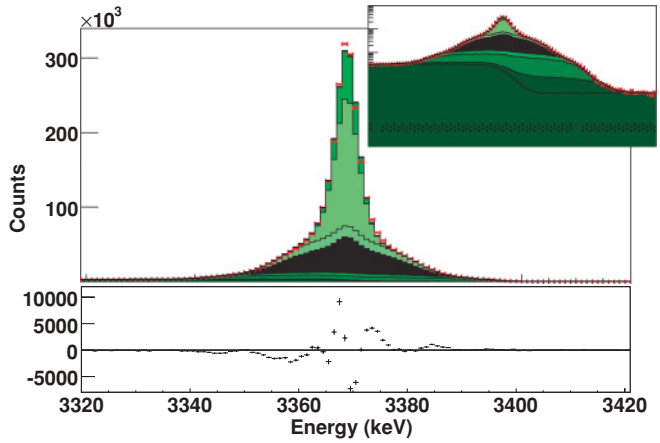

FIG. 14. (Color online) Line-shape analysis of the $2_1^+ \rightarrow 0_1^+$ 3367-keV transition. The best fit is obtained using the parameters given in Table IX. The inset shows the same line shape shown on a log scale to reveal the higher lying neutron contributing branches. In both pictures, the relative contribution of each direct neutron branch is shown using different shades of green, except for the sum of all the indirect contributions shown in black. The difference between the experimental data and the simulation is shown below the figure.

TABLE IX. Line-shape analysis of the $2_1^+ \rightarrow 0_1^+$ 3367-keV transition (see Table VII for an explanation of the data displayed).

$J^\pi = 2_1^+$	$T_{1/2} = 142 \pm 3(\mathrm{stat.}) \pm 7(\mathrm{syst.})$ fs [36]		
From ^{11}Be			
E_{level} (MeV)	E_n (MeV)	ΔE_{max} (keV)	Intensity
3.89	0.02	1.99	9.6(18)
3.96	0.08	4.42	31.8(59)
5.24	1.24	17.44	10.2(17)
7.03	2.87	26.51	4.3(7)
8.03	3.78	30.41	7.3(15)
10.6	6.11	38.69	1.5(3)
From ^{10}Be			
E_{level}(keV)	J^π	BR(%)	
6265.1(5)	2^-	100	6.31(13)
6180.3(5)	0_2^+	65.7(12)	3.02(6)
5961.8(5)	1^-	34(4)	0.89(3)
5958.39(5)	2_2^+	91(2)	25.1(8)
Total			100

V. SUMMARY

In summary, we have studied the β-delayed one-neutron emission of ^{11}Li by analyzing the line shape of the γ transitions observed in ^{10}Be. A summary of all the direct and indirect feedings of excited states in ^{10}Be deduced in this experiment is given in Fig. 15. The half-lives of all but the first excited state of ^{10}Be were measured, and they are compared with other recent measurements and the values listed in the compilation in Table X. Overall, good agreement is found for the 2_2^+ and

TABLE X. Half-lives (in fs) of the ^{10}Be excited states measured in this work and compared with recent studies and values given in the compilation in Ref. [37]. The error given is in some cases the combination of the statistical and systematic errors (see the relevant publications for further detail).

J^π	This work	Fynbo [4]	Sarazin [5]	Tilley [37]
2_2^+	$61.4^{+8.0}_{-6.2}$	>35	60(10)	<55
1^-	44(40)	230(90)	[a]	–
0_2^+	983^{+202}_{-123}	760(170)	870(175)	760^{280}_{210}
2^-	<8	160(40)	85(12)	–

[a]Less than a few hundred fs.

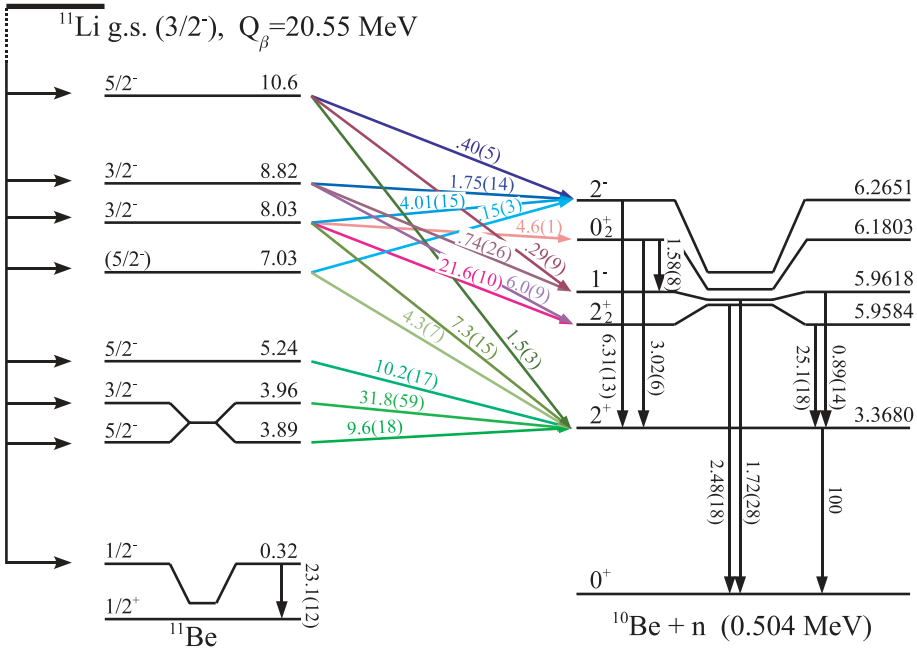

FIG. 15. (Color online) β-delayed one-neutron emission decay scheme of ^{11}Li extracted from this experiment. Intensities given are relative to the intensity of the $2_1^+ \rightarrow 0_1^+$ transition (100). The color scheme refers to the colors used to identify the neutron branches in the figures presenting the line-shape analyses.

0_2^+ states. The half-life of the 1^- state, however, is found to be significantly different from the only other existing measurement [4]. The line-shape analysis of the $2_1^+ \rightarrow 0_1^+$ transition was performed using the 2_1^+ half-life obtained in a recent experiment [36] and is overall in reasonable agreement with Ref. [6], except for the intensities of the two low-lying 3.89- and 3.96-MeV states in ^{11}Be.

The half-life of the 2^- state in ^{10}Be is found to be considerably smaller than previously measured. This can be explained by the increase of contributing neutron branches intervening in the line-shape analysis. The $2^- \rightarrow 2_2^+$ transition strength is now found to be well within the range of both MCM and NCSM calculations and provides further evidence of the halo nature of the 2^- excited state. The 8.82-MeV state in ^{11}Be is found to feed three excited states in ^{10}Be, which are all believed to be built upon a ^{9}Be core plus an s-wave or p-wave neutron. We suggest that this particular state is populated when the β decay of ^{11}Li occurs in its core.

ACKNOWLEDGMENTS

We would like to thank the staff of the ISAC facility for their work in delivering the ^{11}Li beam. This work was partially supported by the US Department of Energy through Grant/Contract Nos. DE-FG03-93ER40789 (Colorado School of Mines) and the Natural Sciences and Engineering Research Council of Canada. TRIUMF receives federal funding via a contribution agreement through the National Research Council of Canada.

[1] D. J. Morrissey *et al.*, Nucl. Phys. **A627**, 222 (1997).
[2] M. J. G. Borge *et al.*, Phys. Rev. C **55**, 8R (1997).
[3] N. Aoi *et al.*, Nucl. Phys. **A616**, 181c (1997).
[4] H. O. U. Fynbo *et al.*, Nucl. Phys. **A736**, 39 (2004).
[5] F. Sarazin *et al.*, Phys. Rev. C **70**, 031302R (2004).
[6] Y. Hirayama *et al.*, Phys. Lett. **B611**, 239 (2005).
[7] I. Tanihata *et al.*, Phys. Rev. Lett. **55**, 2676 (1985); Phys. Lett. **B160**, 380 (1985).
[8] P. G. Hansen and B. Jonson, Europhys. Lett. **4**, 409 (1987).
[9] M. Freer, Rep. Prog. Phys. **70**, 2149 (2007).
[10] J. Al-Khalili and K. Arai, Phys. Rev. C **74**, 034312 (2006).
[11] R. Raabe *et al.*, Phys. Rev. Lett. **101**, 212501 (2008).
[12] P. J. Haigh *et al.*, Phys. Rev. C **79**, 014302 (2009).
[13] C. E. Svensson *et al.*, Nucl. Instr. Methods B **204**, 660 (2003).
[14] G. C. Ball *et al.*, J. Phys. G **31**, S1491 (2005).
[15] H. O. U. Fynbo, Nucl. Instrum. Methods Phys. Res. B **207**, 275 (2003).
[16] J. F. Ziegler and J. P. Biersack, SRIM-2008, http://www.srim.org.
[17] F. Ajzenberg-Selove and J. H. Kelley, Nucl. Phys. **A506**, 1 (1990).
[18] Y. Hirayama *et al.*, Nucl. Phys. **A738**, 201 (2004).
[19] I. Mukha *et al.*, Nucl. Phys. **A616**, 201c (1997).
[20] M. J. G. Borge *et al.*, Nucl. Phys. **A613**, 199 (1997).
[21] P. Mertens and Th. Krist, Nucl. Instrum. Methods **168**, 33 (1980).
[22] L. C. Biedenharn and M. E. Rose, Rev. Mod. Phys. **25**, 729 (1953).
[23] D. C. Radford, Nucl. Instr. Meth. A **361**, 297 (1995).
[24] D. J. Millener, D. E. Alburger, E. K. Warburton, and D. H. Wilkinson, Phys. Rev. C **26**, 1167 (1982).
[25] S. Eidelman *et al.* (Particle Data Group), Phys. Lett. **B592**, 275 (2004).
[26] W. H. Press *et al.*, *Numerical Recipes in C: The Art of Scientific Computing* (Cambridge University Press, New York, 1992).

[27] P. R. Bevington and D. Robinson, *Data Reduction and Error Analysis for the Physical Sciences*, 3rd ed. (McGraw-Hill, New York, 2003), p. 108.
[28] M. Freer *et al.*, Phys. Rev. Lett. **96**, 042501 (2006).
[29] Y. Kanada-En'yo, H. Horiuchi, and A. Doté, Phys. Rev. C **60**, 064304 (1999).
[30] K. Arai, Phys. Rev. C **69**, 014309 (2004).
[31] Y. Ogawa *et al.*, Nucl. Phys. **A673**, 122 (2000).
[32] P. Navrátil (private communication).
[33] N. Itagaki and S. Okabe, Phys. Rev. C **61**, 044306 (2000); N. Itagaki, S. Hirose, T. Otsuka, S. Okabe, and K. Ikeda, *ibid.* **65**, 044302 (2002).
[34] H. Simon *et al.*, Phys. Rev. Lett. **83**, 496 (1999).
[35] E. Caurier, P. Navratil, W. E. Ormand, and J. P. Vary, Phys. Rev. C **66**, 024314 (2002).
[36] E. A. McCutchan *et al.* (submitted to Phys. Rev. Lett.).
[37] D. R. Tilley *et al.*, Nucl. Phys. **A745**, 155 (2004).